

New Type of Self-Organized Criticality in a Model of Erosion

Hideki Takayasu and Hajime Inaoka

Department of Earth Sciences, Kobe University, Kobe 657, Japan

(Received 3 September 1991)

By modeling the process of water erosion we found that river patterns on a surface become invariant after the whole surface is covered by self-organized percolated rivers. Fractal scalings are confirmed in the distribution of basin size and in the contour's geometrical irregularity.

PACS numbers: 64.60.Ht, 05.70.Ln, 68.45.Ws, 92.40.Gc

Mechanisms of creating fractals have been clarified in various fields of science [1-3]. A remarkable success may be the discovery of so-called Laplacian fractals which involve pattern formations in diffusion-limited aggregation, viscous fingering, crystallization, electrodeposition, dielectric breakdown, chemical dissolution, and bacterial colony growth.

Fractal geometry is especially powerful for characterizing random surfaces such as the Earth's relief [4] and porous solids' surfaces [2]. A lot of attention has been paid to random surface growth phenomena which exhibit fractal scalings [5].

Recently, the model of self-organized criticality [6] (SOC), which was introduced as a model of a sandpile, has been attracting much attention because it automatically converges to a statistically steady state where critical or fractal behaviors are found both in space and time. It is anticipated that a large portion of the fractals in nature may be created by this kind of self-organization.

In this paper we analyze surfaces under water erosion. We will show that a surface spontaneously evolves into a kind of critical state characterized by fractal scalings. The critical state is very different from that of the SOC model in that the patterns of water flows (i.e., river patterns) on the surface are frozen, namely, they do not change after the system reaches the critical state. Thus we have critical behavior only in space.

Landscapes and river patterns are familiar to everybody but they have not attracted many physicists' interest so far. Mandelbrot first showed that coastlines can be characterized by fractal dimensions [5]. He also graphically demonstrated that the Earth's relief is a fractal by proposing fractional Brownian surfaces as landscapes. Although the resulting surfaces look natural at first sight, there is an obvious flaw, that is, no river exists on the surface.

River patterns are also known to be typical fractals [3,4]. Scheidegger proposed a lattice model of rivers which is defined on a slope where water on a site flows randomly to either the left down site or the right down site [7]. His river model was shown to be identical to the one-dimensional random particle aggregation model with uniform injection by regarding the direction of the slope as the time axis [8]. The model is known to show critical behavior automatically like the SOC model; for example, it was proved that the system converges to a steady state

where the distribution of the drainage basin area or particle mass rigorously follows a power law [9].

For the creation of real river patterns and landscapes we believe that the effect of water erosion should play the central role. By this motivation we model the erosion process on a lattice and simulate the formation of river patterns.

The model is defined on a two-dimensional triangular lattice. Each site has two variables, $h(x,y)$, the height of the Earth's surface, and $s(x,y)$, the water flow intensity. For a given initial configuration time evolution is performed according to the following procedures.

(1) *Rain fall.*—We assume that rain falls constantly on every site in the amount of $s_0 (=1)$.

(2) *Water flow.*—For every site (x,y) we find the lowest value of height in the six nearest neighbors, $\min\{h(x',y')\}$, where (x',y') denotes a nearest-neighbor site. The water at (x,y) flows to the lowest neighbor if the destination's height is lower than $h(x,y)$. Applying this procedure for all sites we can draw a global water flow pattern as shown in Fig. 1, which we call a river pattern. The flow intensity $s(x,y)$ is defined by the sum of water flows from neighbors and the rain fall on the site; so, when the river pattern becomes stationary all rain to the upstream of (x,y) gathers at (x,y) , and $s(x,y)$ is equal to the size of the drainage basin area for the site (x,y) . (We treat local minimum sites in a separate way as described later.)

(3) *Water erosion.*—By the effect of erosion the height at (x,y) is decreased by $\delta h(x,y) = F(J(x,y))[h(x,y) - \min\{h(x',y')\}]$, where $J(x,y)$ is the water power which is defined as

$$J(x,y) \equiv s(x,y)[h(x,y) - \min\{h(x',y')\}]. \quad (1)$$

The function F is a positive and monotonically increasing function which characterizes the erosion. In the following simulation $F(J) = C_1 J / (C_2 + J)$, where C_1 and C_2 are positive constants. In this paper we use $C_1 = 0.5$ and $C_2 = 100$.

(4) *Repeat the above procedures.*—Procedures (1), (2), and (3) constitute one time step.

As seen from the above procedures we assume that the water is supplied only by rain and is conserved in the flow process. We neglect the accumulation of sand, so $h(x,y)$ decreases monotonically.

In procedure (2) we have to treat the local minimum

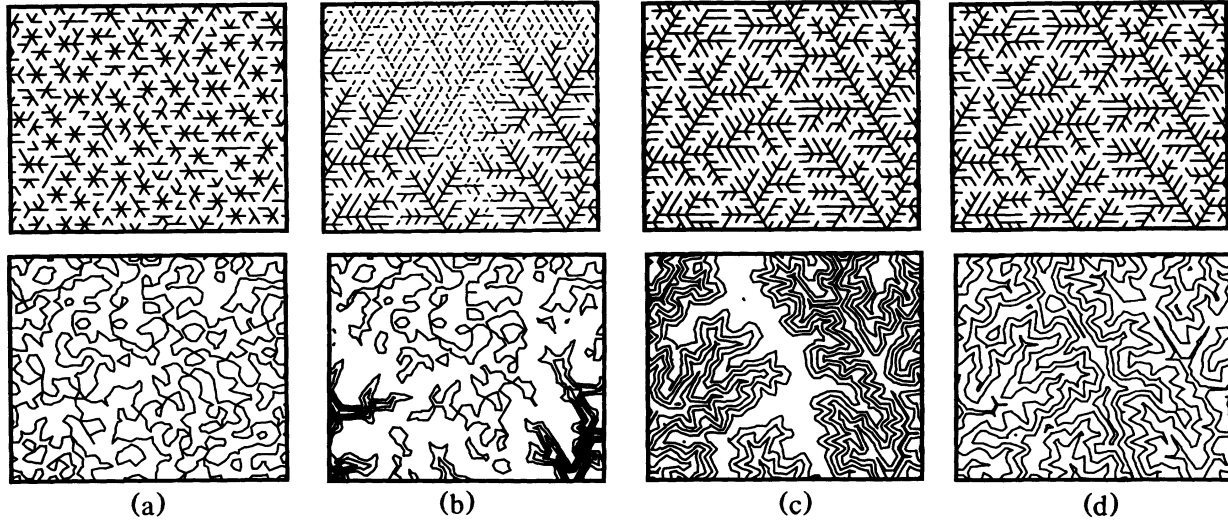


FIG. 1. Time evolution of river patterns (above) and contours (below). (a) The initial condition. $h(x,y) = 2000 + N_{rnd}$, where N_{rnd} is a uniform random number in the interval $[0,0.1)$, $s(x,y) = 0$, and $w(x,y) = 0$. (b) At 300 time steps. The dashed parts of the river pattern show lakes where water accumulation is not zero. (c) At 600 time steps. (d) At 1000 time steps.

sites separately because water does not flow out at those points. Intuitively we can expect the following evolution for those sites. A local minimum site and its basin sites make a lake and water accumulates until it flows out from the edge of the lake. Then the edge is eroded intensively and finally the lake vanishes. In order to realize this scenario we apply the following additional rules.

(a) We introduce a new quantity, $w(x,y)$, the height of water accumulation for the local minimum sites and their basins, which is defined as

$$w(x,y) \equiv \min\{h(x',y')\} - h(x,y) + \epsilon, \tag{2}$$

where ϵ is a very small positive number; in our simulation $\epsilon = 0.1$.

(b) The height function $h(x,y)$ is replaced by

$$h'(x,y) \equiv h(x,y) + w(x,y), \tag{3}$$

and the above evolution procedures are applied for $h'(x,y)$.

(c) The function $w(x,y)$ vanishes when $\min\{h(x',y')\}$ becomes smaller than $h(x,y)$.

Note that all time evolution rules are deterministic, so randomness comes only from the initial condition.

An example of time evolution starting from a nearly flat surface with small uniform random fluctuation is shown in Fig. 1. Here, we are observing a part (30×30) of the system of size 100×100 with periodic boundaries for the left and right edges and with fixed boundaries for the top and bottom edges. The bottom edge is much lower than the top edge, so water flows out only from the bottom edge. Accordingly river patterns and contours grow from the bottom to the top. We find the growth of river patterns from the early disconnected stage [Fig. 1(a)] to the fully developed space-filling stage [Fig.

1(d)].

In Fig. 2 we plot the number density of sites which belong to lakes together with the number of flows which change direction in one time step. As seen from the figure almost all sites are lakes in the beginning due to the initial condition. The number of lake sites decreases nearly constantly and no lake remains after about $t = 2000$. At this time all rivers have percolated to the boundary and all of the rain water is drained out without any accumulation. Water flow directions are unstable in and around a lake especially when water begins to flow out from the lake's edge. As seen from Fig. 2 the number of unstable flows also decreases monotonically and it becomes negligibly small a little before the time that all lakes have vanished. We focus our attention on this stationary state and analyze its statistical properties.

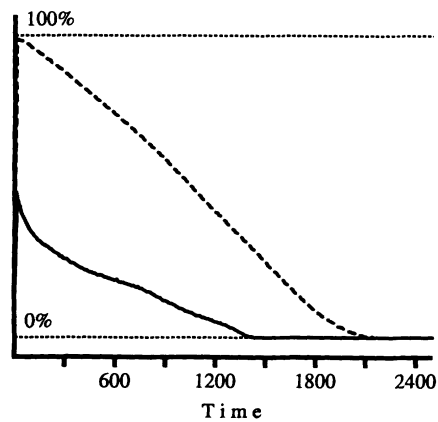


FIG. 2. Time evolution of number of lake sites (dashed line) and number of unstable flows which change direction in one step (bold line). The number is shown in percentiles.

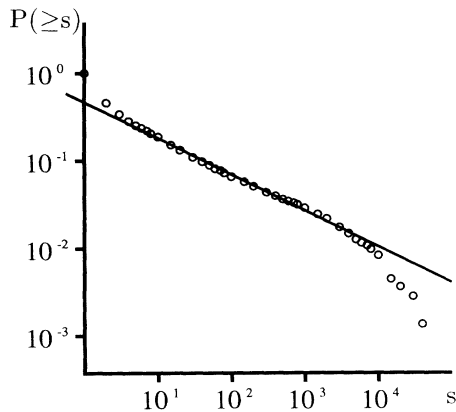


FIG. 3. The cumulative distribution of flow intensity, $P(\geq s)$, on a log-log scale. The line shows the power law $s^{-0.41}$.

In Fig. 3 the flow intensity distribution is plotted on a log-log scale for a system of size 512×512 with 5000 time steps. Here $P(\geq s)$ denotes the probability that the water flow intensity of a randomly chosen site is larger than s . As this is observed in the steady state the distribution is equivalent to the drainage-basin size distribution. The points are clearly on a straight line for the range from $s=10^1$ to 10^3 , which demonstrates a critical property of the steady state. For s larger than 10^4 the distribution decays exponentially due to the finite size of the system. By comparing results of different system sizes we estimate the distribution in an infinite system as

$$P(\geq s) \propto s^{-\beta}, \quad \beta=0.40. \quad (4)$$

This exponent is significantly larger than the value of Scheidegger's model [10], $\frac{1}{3}$, and is nearly equal to the exponent for the branch size distribution for diffusion-limited aggregation in two-dimensional space [10].

Although the river patterns are stationary in the steady state, the contours keep changing because the surface is always eroded by the water flow. Actually the river patterns in Figs. 1(c) and 1(d) are nearly identical but the corresponding contours look very different. In the steady state the snapshot shape of the contours can be characterized by the fractal dimension. By using the box counting method we confirm power-law scalings over nearly two decades of scale length. The value of the contours' fractal dimension is estimated as $D=1.60 \pm 0.15$, which seems to depend slightly on both height and time steps.

In order to see the dependence of the exponent and fractal dimension on the erosion function we generalize the erosion function as $F(J)=C_1 J^a/(C_2^2+J^a)$. Our numerical results for $a=2$ and 3 are as follows: The river patterns are frozen after all lakes have vanished. In the steady state the drainage-basin distribution follows the same power law as Eq. (4) for any a within error bars. The fractal scaling of the contours also holds in the gen-

TABLE I. The exponent of distribution of drainage basin area, β , and the fractal dimension of contour lines, D , for different a .

a	1	2	3
β	0.41	0.41	0.41
D	1.60	1.45	1.35

eralized cases but with different values for the dimension (see Table I). Intuitively speaking, we have thinner and steeper valleys for larger a . It is interesting that the dimensions are close to those for Laplacian fractals with growth probability proportional to the a th power of potential gradients [11] ($D=1.5$ and 1.4 for $a=2$ and 3 , respectively).

Real river patterns are known to satisfy Horton's laws [12]. We confirm the validity of the laws for our steady-state river patterns and estimate the values $R_B=5.3$ for the bifurcation ratio and $R_L=2.7$ for the stream length ratio in the case of $a=1$ [13]. The ranges of values for natural drainage basins are known to be [14] $2 \leq R_B \leq 6$ and $1.5 \leq R_L \leq 3.5$. Recently, Stark [15] proposed a model of river patterns created by self-avoiding invasion percolation and estimated the intrinsic fractal dimension of the stream network as 1.68 by using La Barbera and Rosso's formula [14], $D=\log R_B/\log R_L$. By applying this formula, we obtain the same value $D=1.68$ for our model.

More detailed analyses, including the dependence of the results on the model parameters, the sensitivity to the initial condition, a mean-field-type theory, and comparison with real landscapes, are now in progress.

We would like to acknowledge the Rikei Corporation for the opportunity to use a Massive Parallel SIMD computer, MasPar MP-1204.

- [1] J. Feder, *Fractals* (Plenum, New York, 1988); T. Vicsek, *Fractal Growth Phenomena* (World Scientific, Singapore, 1989).
- [2] *The Fractal Approach to Heterogeneous Chemistry*, edited by D. Avnir (Wiley, New York, 1989).
- [3] H. Takayasu, *Fractals in the Physical Sciences* (Manchester Univ. Press, Manchester, 1990).
- [4] B. B. Mandelbrot, *The Fractal Geometry of Nature* (W. H. Freeman, San Francisco, 1982).
- [5] See, for example, M. Kardar, G. Parisi, and Y.-C. Zhang, *Phys. Rev. Lett.* **64**, 543 (1990).
- [6] P. Bak, C. Tang, and K. Wiesenfeld, *Phys. Rev. Lett.* **59**, 381 (1987); *Phys. Rev. A* **38**, 364 (1988).
- [7] A. E. Scheidegger, *Bull. I.A.S.H.* **12** (1), 15 (1967).
- [8] H. Takayasu, I. Nishikawa, and H. Tasaki, *Phys. Rev. A* **37**, 3110 (1988); H. Takayasu, *Phys. Rev. Lett.* **63**, 2563

- (1989).
- [9] G. Huber, *Physica (Amsterdam)* **170A**, 463 (1991); H. Takayasu, M. Takayasu, A. Provata, and G. Huber, *J. Stat. Phys.* (to be published).
- [10] H. Takayasu, *J. Phys. Soc. Jpn.* **57**, 2585 (1988).
- [11] K. Honda, H. Toyoki, and M. Matsushita, *J. Phys. Soc. Jpn.* **55**, 707 (1986).
- [12] R. E. Horton, *Bull. Geol. Soc. Am.* **56**, 275 (1989).
- [13] H. Inaoka and H. Takayasu (to be published).
- [14] P. La Barbera and R. Rosso, *Water Resour. Res.* **25**, 735 (1989).
- [15] C. P. Stark, *Nature (London)* **352**, 423 (1991).